JOURNAL OF MATERIALS SCIENCE 23 (1988) 3550–3557

Creep of (Mg, Fe)O single crystals

J. WOLFENSTINE, D. L. KOHLSTEDT
Department of Materials Science, Cornell University, Ithaca, New York 14853, USA

The creep behaviour of (Mg, Fe)O single crystals compressed along ⟨1 0 0⟩ has been investigated over the temperature range 1300 to 1500° C, at stresses between 20 and 70 MPa, for oxygen partial pressures between 10^{-4} and 10^{2} Pa, and with iron concentrations between 70 and 11 900 p.p.m. Under these conditions, the dependence of the steady-state strain rate on stress, temperature, oxygen partial pressure, and iron concentration can be summarized by the flow law, $\dot{\varepsilon} = A\sigma^{3.4}[Fe_{Mg}]_{tot}^{0}P_{O_2}^{0} \exp(-445\,kJ\,mol^{-1}/RT)$. These results suggest that the steady-state strain rate is controlled by dislocation climb with a jog velocity which is limited by lattice diffusion of oxygen by a vacancy pair mechanism. The activation energy for creep, 445 kJ mol^{-1} is larger than that reported for self-diffusion of oxygen, 330 kJ mol^{-1}, because the formation energy for jogs is relatively large, 115 kJ mol^{-1}.

1. Introduction

Magnesium oxide (MgO) is often considered a model ceramic material, because of its simple rocksalt structure, whose elevated melting point (T_m = 2800° C) and general availability make possible many high-temperature applications. Thus, the creep properties of MgO are of interest. Over the last twenty-five years, there have been a number of high-temperature creep studies on undoped and doped single crystals of MgO to determine the rate-controlling creep mechanism(s) [1–12]. These investigations have concentrated on identifying the creep mechanism(s) by measuring the dependence of the steady-state strain rate on stress and temperature. However, in the case of MgO doped with the transition metal impurities nickel, cobalt, and iron, the concentrations of point defects and, thus, the creep rate may also depend upon the oxygen partial pressure and dopant concentration. It is the intent of this study to place constraints on the possible rate-controlling mechanism(s) for the creep of (Mg, Fe)O single crystals by investigating the dependence of the steady-state strain rate on oxygen partial pressure and dopant concentration as well as on stress and temperature.

In general, the steady-state creep of a non-stoichiometric solid-solution oxide single crystal, such as (Mg, Fe)O, can be represented by an equation of the form

$$\dot{\varepsilon} = A\sigma^{n} P_{O_2}^{m}[Fe_{Mg}]_{tot}^{q} \exp(-Q/RT) \quad (1)$$

where $\dot{\varepsilon}$ is the steady-state strain rate, A a materials parameter, σ the applied stress, n the stress exponent, P_{O_2} the oxygen partial pressure, m the oxygen partial pressure exponent, $[Fe_{Mg}]_{tot}$ the total iron concentration in solid solution, q the concentration exponent, Q the activation energy for creep, R the universal gas constant, and T the absolute temperature. The rate-controlling creep mechanisms are usually identified by comparing the experimental values of n, m, q, and Q with those predicted by theory.

For single crystal MgO at $T > 0.5T_m$, it can be assumed that the steady-state creep rate is controlled either by dislocation glide or by dislocation recovery via a diffusion-controlled climb mechanism. The likelihood that the compressional creep of single crystal MgO at $T > 0.5T_m$ is rate-limited by dislocation climb rather than dislocation glide is suggested by the subgrain structures, dislocation networks within the subgrains, and the absence of long straight dislocations [6, 7, 13, 14]. The deformation experiments of Birch and Wilshire [7, 8], who investigated the effects of stress-reductions during creep, help to confirm the climb mechanism. After a reduction in the stress level on a single crystal of MgO, an incubation period (i.e., a period of zero creep rate) was observed before creep commenced at the lower stress level. If dislocation glide is rate-controlling, the incubation period should be absent. Also, if a glide is rate controlling, the creep rate should be very sensitive to the impurity concentration. The high-temperature experiments of Moon and Pratt [15] and of Reppich [16] indicate that deformation of MgO crystals is insensitive to the concentration of divalent or trivalent cation impurities. Consequently, at high-temperature ($T > 0.5T_m$) the creep of MgO single crystals appears to be controlled by dislocation climb.

Dislocation climb involves the transport of matter by diffusion. In a compound such as MgO/(Mg, Fe)O, this transport has to preserve stoichiometry; as a consequence, both cations and anions must diffuse to the dislocation to allow climb to occur. If the dislocation is a perfect source or sink for defects, then the creep rate should be controlled by the diffusion of the slowest species. In single crystals of (Mg, Fe)O and MgO, lattice diffusion of oxygen is much slower than lattice diffusion of the cations [17]. The values of m, q and/or Q measured from creep experiments on (Mg, Fe)O and/or undoped MgO can be compared to measured and theoretical values for lattice self-diffusion of oxygen. This comparison can permit

0022–2461/88 $03.00 + .12

TABLE I Chemical analysis of crystals (p.p.m.)

Element	Norton	Spicer 4N	Spicer 3N	Tateho
Al	45	35	30	20
Ca	280	50	2480	45
Cd	< 1	< 1	< 1	< 1
Co	3	5	10	3
Cu	1	1	20	15
K	10	5	3	5
Mn	22	35	47	10
Mo	< 1	< 1	< 1	< 1
Ni	15	18	12	15
Pb	< 1	< 1	< 1	< 1
Zn	2	1	5	1

identification of the point defects responsible for controlling the creep rate, since diffusion of a species requires the movement of point defects.

2. Background

2.1. Mechanical properties of iron doped MgO

The mechanical properties of iron-doped MgO can be very sensitive to the form and distribution of the iron. In single crystals of MgO, iron substitutes for Mg^{+2} as either Fe^{+3} or Fe^{+2}. The Fe^{+2} to Fe^{+3} ratio depends upon temperature, P_{O_2}, and total iron content [15]. Iron can also be present in second phase precipitates of $MgFe_2O_4$ or metallic iron [15]. Previous investigations of the mechanical properties of iron-doped MgO single crystals have focused on solid-solution hardening. Precipitation hardening of MgO containing Fe^{+3} has also been investigated.

MgO single crystals have shown that at relatively low temperatures ($T < 0.5T_m$), Fe^{+3} strongly hardens MgO, while Fe^{+2} had little effect on the yield strength [18–21]. In contrast, at temperatures above 1300° C, the yield strength of iron-doped MgO approaches that for undoped MgO [15, 16] and is insensitive to the type and concentration of impurities [11].

Precipitation hardening in iron-doped MgO has been investigated by Groves and Fine [18], Srinivasan and Stoebe [20], Kruse and Fine [21], and Ilschner and Reppich [15]. They observed that heat-treatments produced $MgFe_2O_4$ precipitates in a (Mg, Fe)O matrix which had room-temperature yield strengths that were three to five times greater than the room-temperature yield strength of undoped MgO containing no $MgFe_2O_4$ precipitates. The strengthening was attributed to stacking faults in the particles and to the particle–matrix surface that was created when dislocations cut the particles [21].

3. Experimental

3.1. Sample characterization

Single crystals of MgO were obtained from Norton Co. (Niagara Falls, Canada), Tateho Co. (Hyogo-Ken, Japan), and W. C. Spicer Ltd (Cheltenham, England). The undoped MgO was from Norton, while the intentionally iron-doped crystals were from Spicer and Tateho.

The impurity content of the crystals was determined by flame emission spectroscopy at Cornell University and, except for the iron content, is listed in Table I.

TABLE II Iron concentration of the crystals (p.p.m.)

Source	Fe
Norton	70
Spicer 4N	11 900
	4 300 (4 725)
Spicer 3N	710 (706)
	300
Tateho	1 500

The iron content of the crystals determined by flame emission spectroscopy at Cornell University and that quoted by the supplier, are given in Table II; the two values are in good agreement. The iron content of our crystals ranged from 70 to 11 900 p.p.m.

3.2. Sample preparation

Rectangular parallelopiped deformation specimens were oriented by Laue X-ray back reflection so that the faces were parallel to {1 0 0}, then cleaved or cut with a low speed diamond saw to typical dimensions of 2 mm × 2 mm × 4 mm. The specimens were next ground on 600 grit SiC paper and polished on a silk cloth with 6 μm diamond paste to ensure that the ends of the specimens were parallel to each other and perpendicular to the side faces.

To ensure that the iron was present in solid solution and not in precipitates, the iron-doped crystals were heated prior to deformation within the (Mg, Fe)O stability field [22] at 1400° C for 100 h at a P_{O_2} of 10^{-3} Pa and cooled to room temperature at rate of 400° C h^{-1} at a P_{O_2} of 10^{-3} Pa. Crystals that were coloured orange or brown, characteristic of $MgFe_2O_4$ precipitates [19, 20], prior to the heat-treatment were clear or green after the heat-treatment, indicating that $MgFe_2O_4$ precipitates had redissolved and that iron was present as ions, Fe^{+3} or Fe^{+2}, substituting for Mg^{+2} [19, 23].

3.3. Creep testing

Samples were deformed at stresses between 20 and 70 MPa in uniaxial compression at constant stress. The load was applied parallel to ⟨1 0 0⟩. The creep apparatus was a dead-load type in which the load is transmitted from the loading head to the sample via SiC pistons. The bottom piston is rigidly attached to the frame. The sample shortening was measured with two direct current displacement transducers (DCDTs), diametrically opposite each other, which measure the motion of the top piston relative to the fixed bottom piston. The summed output was recorded on a chart recorder.

In an effort to keep the stress constant, load adjustments were made after each 1% strain during the experiments. The magnitude of the load adjustment was calculated assuming that the deformation was homogeneous and that the volume of the sample remained constant throughout the experiment [24]. The axial strain determined by micrometer measurements on the specimen before and after testing agreed with values determined from the chart record. The SiC platens which separated the pistons from the sample were not indented. However, a thin reaction layer

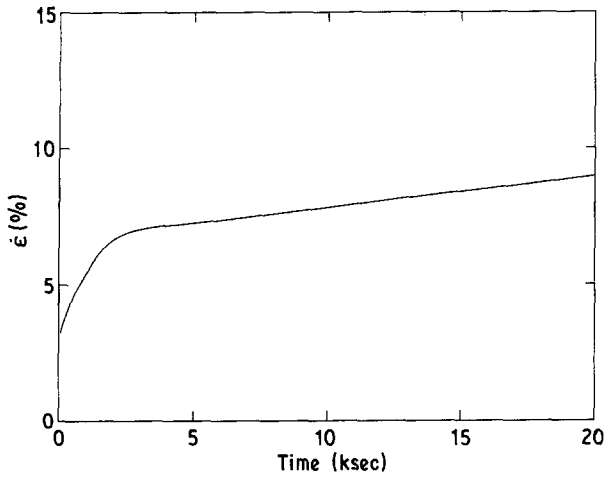

Figure 1 Creep curve for one (Mg, Fe)O single crystal. Iron concentration 4300 p.p.m., $T = 1400°C$, $\sigma = 50$ MPa.

formed between the sample and the platens. The deformation is given in terms of true strain.

Deformation experiments were conducted over the temperature range 1300 to 1500° C. Temperatures up to 1450° C were reached using a furnace heated by Kanthal Super 33 elements. The temperature was measured using a platinum–Pt13%Rh thermocouple located within 15 mm of the sample. Thermal profile experiments indicated that temperature differences between the specimen and the thermocouple were less than 1° C [25]. For temperatures between 1450 and 1500° C, a tungsten-mesh heating element was used. Here, the temperature was measured using a W5%Re–W26%Re thermocouple located within 1 cm of the sample. The temperature differences between the specimen and the thermocouple was less than 2° C. The samples were heated/cooled at 350° C h^{-1}. On cooling at the end of each creep run, the load was kept on the specimen until the temperature reached 1000° C after which the load was removed. With this procedure the equilibrium microstructure established during the high-temperature creep experiment is retained [26].

The specimen and pistons were surrounded by a mullite muffle tube through which either argon ($P_{O_2} = 3 \times 10^{1}$ Pa) or CO/CO_2 gas mixtures were passed to control the P_{O_2}. The oxygen partial pressure

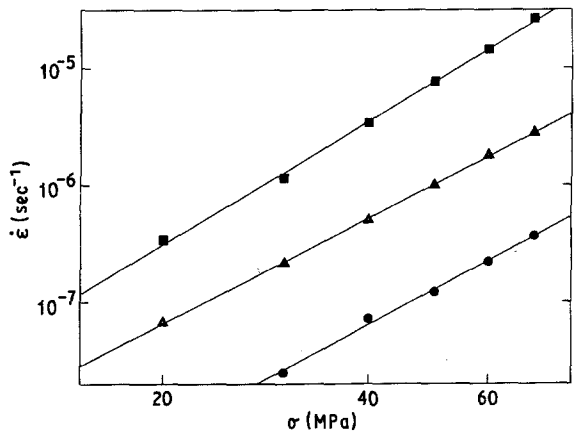

Figure 2 Steady-state strain rate plotted against stress for undoped MgO. (● $T = 1300°C$, ▲ $T = 1400°C$, ◆ $T = 1500°C$) $n = 3.4 \pm 0.3$.

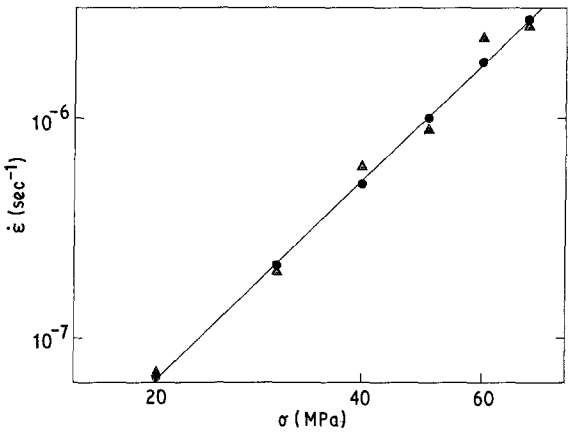

Figure 3 Steady-state strain rate plotted against stress for iron-doped (▲) and undoped (●) MgO. $n = 3.2$, $T = 1400°C$.

range used for the experiments from 10^{-4} to 10^{2} Pa, was within the (Mg, Fe)O stability field [22]. The CO/CO_2 gases were mixed using calibrated flowmeters with an attached mixing chamber. The P_{O_2} of the gases was measured with a calcia-stabilized zirconia sensor attached to the exhaust line. The P_{O_2} in the sample chamber reequilibrated within 30 min following changes in the gas mixture [24]. After a P_{O_2} change, the sample was held at the new P_{O_2} for 3 to 5 h to allow point defect concentrations in the sample to reach their new equilibrium values.

To obtain information about the creep mechanism(s), the parameters, n, m, q, and Q of the creep equation, Equation 1, were determined by changing either σ, T, $[Fe_{Mg}]_{tot}$, or P_{O_2} while leaving the other three unchanged.

4. Results

A typical creep curve for a (Mg, Fe)O single crystal deformed at 1400° C under a constant stress of 50 MPa is shown in Fig. 1. After the instantaneous elastic strain which occurs on application of the load, there is a period of transient creep, during which the creep rate decreases continuously with increasing time. Finally, after a true strain of 7.5%, a steady-state period is reached in which the creep rate remains essentially constant. For most samples, the creep tests were continued for a total true strain of 18 to 25%. After true strains of about 10%, barrelling of the sample was detected.

Steady-state strain rate is plotted as a function of stress in Figs 2 and 3. For undoped MgO, a value of $n = 3.4 \pm 0.3$ was obtained by averaging values of n, calculated from a least squares fit for data obtained at three temperatures, Fig. 2. The dependence of the steady-state creep rate on stress is approximately the same for undoped and iron-doped MgO, Fig. 3.

The steady-state strain rate as a function of inverse temperature for undoped and iron-doped MgO at stresses of 30 and 50 MPa is shown in Fig. 4. The activation energy for creep, $Q = 445 \pm 15$ kJ mol^{-1}, was obtained by averaging the least-squares values at each composition for the two stresses. Data for two iron concentrations are shown.

The effect of P_{O_2} on the steady-state creep rate for the MgO samples containing the highest iron

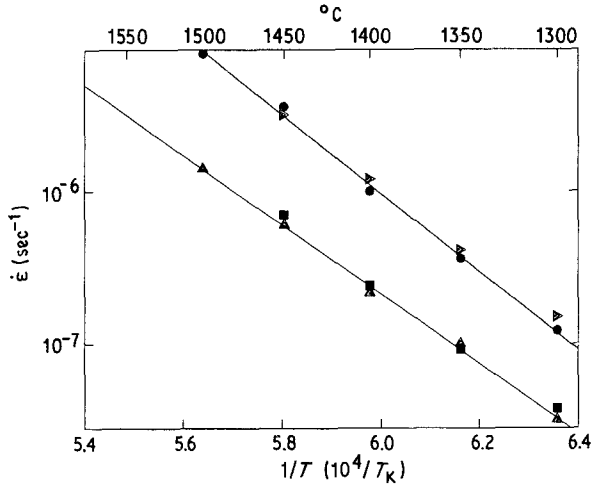

Figure 4 Steady-state strain rate plotted against $1/T$ for iron-doped (▶σ = 30 MPa, 11 900 p.p.m., ▲ 50 MPa, 4300 p.p.m.) and undoped (●σ = 30 MPa, ■σ = 50 MPa) MgO. Q = 445 ± 15 kJ mol^{-1}.

concentration is illustrated in Fig. 5. The creep rate is insensitive to changes in P_{O_2}, giving an oxygen partial pressure exponent, $m \approx 0$.

The effect of iron concentration on the steady-state creep rate is shown in Fig. 6. The creep rate is independent of iron concentration, consistent with the data presented in Figs 2 and 5.

The dependence of the steady-state creep rate on P_{O_2}, iron content, temperature, and stress can be summarized by substituting the experimentally determined values of n, m, q, and Q into Equation 1, which becomes

$$\dot{\varepsilon} = A\sigma^{3.4}[Fe_{Mg}]^0_{tot}P^0_{O_2} \exp(-445\,\text{kJ mol}^{-1}/RT) \quad (2)$$

The raw experimental data for creep of (Mg, Fe)O are reported in Table III.

5. Discussion

5.1. Present experiments

To discuss the result given in Equation 2 in terms of a rate-controlling mechanism for creep, two important criteria must be satisfied. First, are the deformation experiments conducted in a region where the extrinsic vacancy concentration is controlled by Fe^{+3} and not by other trivalent cation impurities such as aluminium and chromium? Second, has the sample

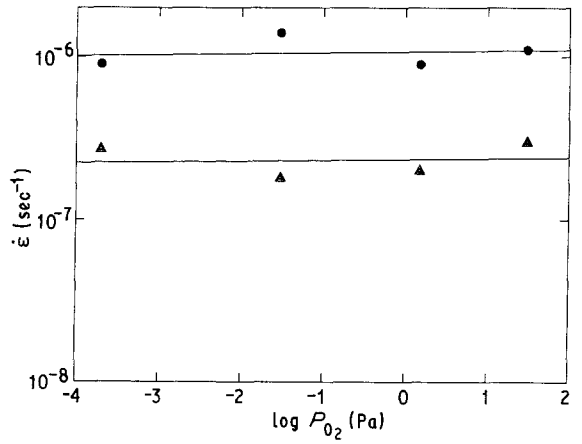

Figure 5 Steady-state strain rate plotted against partial pressure for iron-doped (11 900 p.p.m.) MgO. T = 1400° C (● 50 MPa, ▲ 30 MPa).

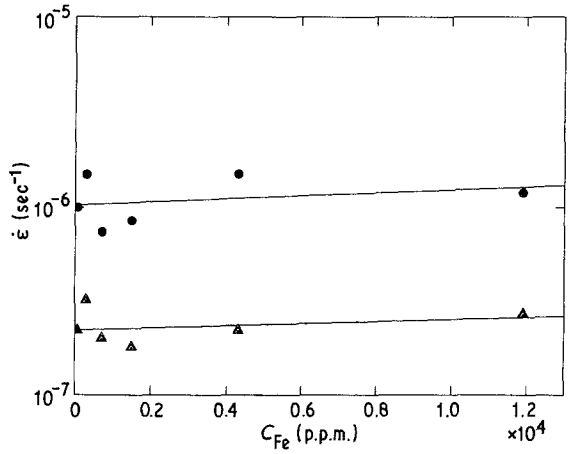

Figure 6 Steady-strain rate plotted against iron concentration T = 1400° C (● 50 MPa, ▲ 30 MPa).

been given enough time to reach thermodynamic equilibrium after a change in P_{O_2} or temperature?

As the iron-doping levels are low in the MgO, aliovalent "background" impurities could possibly be the majority point defects. In MgO, the most common aliovalent cation impurities are Al^{+3}, Cr^{+3}, and Si^{+4}. Calculations by Gourdin *et al.* [27] indicate that Si^{+4} and its compensating cation vacancies are completely associated at temperatures of 1400° C. Hence, they do not affect the concentration of free cation vacancies. The total concentration of Al^{+3} and Cr^{+3} in the (Mg, Fe)O single crystals ranges from 40 to 80 p.p.m., Table I. In the worst case, assume that the total concentration of Al^{+3} plus Cr^{+3} is approximately 100 p.p.m. (see Table I) and that all the extrinsic cation vacancies are unassociated. The concentration of free extrinsic cation vacancies can be determined using the charge neutrality condition

$$\sum z_i c_i = 0 \quad (3)$$

where z_i is the charge of the species and c_i is the concentration of the species. For Al^{+3} and Cr^{+3} in MgO, Equation 3 becomes

$$[F^{\cdot}_{Mg}] = 2[V''_{Mg}]_{imp} \quad (4)$$

with F = Al^{+3} and Cr^{+3}. The Kroger–Vink notation is used in Equation 4, so that the charges are measured relative to a neutral lattice. $F^{\cdot}_{Mg}$ is a foreign metal ion on a magnesium ion site with an effective positive charge, and V''_{Mg} is a vacant magnesium site with an effective double negative charge. Hollenberg and Gordon [28] have shown that the concentration of cation vacancies due to Al^{+3} and Cr^{+3}, $[V''_{Mg}]_{imp}$, determined by Equation 4 is not a function of P_{O_2}.

The results of Moon and Pratt [15] and of Reppich [16] at $T > 1350$° C indicate that all of the extrinsic cation vacancies due to Fe^{+3} are free. If Fe^{+3} is the major aliovalent impurity present in MgO, the charge neutrality condition is

$$[Fe^{\cdot}_{Mg}] = 2[V''_{Mg}]_{Fe} \quad (5)$$

Where $Fe^{\cdot}_{Mg}$ represents an Fe^{+3} ion on a magnesium ion site. The concentration of Fe^{+3}, which is a function of temperature, P_{O_2}, and total iron concentration, was determined using the results of Gourdin *et al.* [27]. In Fig. 7, the extrinsic cation vacancy concentration,

TABLE III Summary of creep data for (Mg, Fe)O

σ (MPa)	T (°C)	Fe (p.p.m.)	P_{O_2} (Pa)	$\dot{\varepsilon}$ (sec^{-1}) ($\times 10^{-7}$)
20	1500	70	32	3.4
30	1500	70	32	12
40	1500	70	32	34
50	1500	70	32	77
60	1500	70	32	150
70	1500	70	32	270
20	1400	70	32	0.17
30	1400	70	32	2.2
40	1400	70	32	5.0
50	1400	70	32	10
60	1400	70	32	18
70	1400	70	32	28
30	1300	70	32	0.25
40	1300	70	32	0.72
50	1300	70	32	1.2
60	1300	70	32	2.2
70	1300	70	32	3.7
20	1400	4300	32	0.78
30	1400	4300	32	2.0
40	1400	4300	32	6.0
50	1400	4300	32	8.8
60	1400	4300	32	23
70	1400	4300	32	27
50	1500	4300	32	78
50	1450	4300	32	35
50	1400	4300	32	10
50	1350	4300	32	3.6
50	1300	4300	32	1.2
30	1450	11900	32	7.0
30	1400	11900	32	2.4
30	1350	11900	32	0.92
30	1300	11900	32	0.38
50	1400	11900	32	11
50	1400	11900	1.5	9.0
50	1400	11900	0.03	14
50	1400	11900	0.002	9.0
30	1400	11900	32	3.0
30	1400	11900	1.5	2.3
30	1400	11900	0.03	2.7
30	1400	11900	0.002	2.6
50	1400	70	32	40
50	1400	300	32	15
50	1400	710	32	7.4
50	1400	1500	32	8.5
50	1400	4300	32	15
50	1400	11900	32	12
30	1400	70	32	2.2
30	1400	300	32	2.0
30	1400	710	32	1.8
30	1400	1500	32	2.2
30	1400	4300	32	2.5
30	1400	11900	32	2.3

calculated using Equation 4, $[V''_{Mg}]_{imp}$, and the extrinsic cation vacancy concentration calculated using Equation 5, $[V''_{Mg}]_{Fe}$, as well as their sum, $[V''_{Mg}]_{tot}$, are plotted against the total iron concentration at a fixed temperature and P_{O_2}. The value of the P_{O_2}, 1 Pa, is in the middle of the stability field. At iron concentrations below 800 p.p.m., the total cation vacancy concentration is controlled by the Al^{+3} and Cr^{+3} impurities. At iron concentrations, above about 2000 p.p.m., the total cation vacancy concentration is essentially fixed by the Fe^{+3} concentration.

In Fig. 8 the extrinsic cation vacancy concentrations, calculated using Equations 4 and 5, plus their sum are plotted against P_{O_2} at fixed total iron concentration and temperature. In this case, a total iron concentration of 4 300 p.p.m. was used, which corresponds to the MgO crystal with the second highest doping level. For P_{O_2} less than 10^{-4} Pa the total vacancy concentration is controlled by impurities (Al^{+3} + Cr^{+3}). For P_{O_2} greater than 10^{-4} Pa, the total cation vacancy concentration is essentially fixed by the Fe^{+3} concentration. In Fig. 9, a similar plot is presented for the MgO crystal doped with 11 900 p.p.m. iron. The total cation vacancy concentration is controlled by the Fe^{+3} concentration over the whole P_{O_2} range; The Al^{+3} and Cr^{+3} impurities have essentially no effect. In answer to the first question, then, Figs 7, 8, and 9 confirm that at least crystals with 4 300 and 11 900 p.p.m. iron were deformed over the entire P_{O_2} range in a region where the total cation vacancy concentration is controlled by the Fe^{+3} concentration and not by the Al^{+3} and Cr^{+3}. At the higher P_{O_2} used in this study, crystals with the lower iron concentrations (i.e., 300, 710, and 1.500 p.p.m.) were also deformed in a region where the total cation vacancy concentration is controlled by the Fe^{+3} concentration and not by the Al^{+3} and Cr^{+3}.

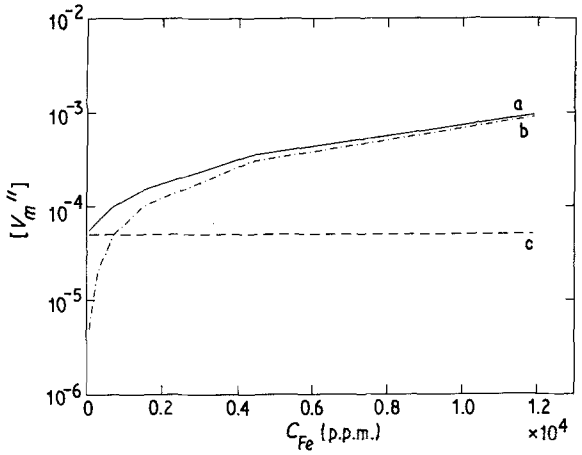

Figure 7 Extrinsic cation vacancy concentration plotted against iron concentration. T = 1400° C, P_{O_2} = 1 Pa (a $[V''_m]_{tot}$, b $[V''_m]_{Fe}$, c $[V''_m]_{imp}$).

Second, has the sample had enough time to reach thermodynamic equilibrium after a change in P_{O_2}? (Mg, Fe)O is a p-type semiconducting material. Thus, while the anionic sublattice has a very low concentration of point defects (probably $< 10^{-6}$) over wide ranges of temperature and oxygen partial pressure, the cationic sublattice contains a significant concentration (probably $\approx 10^{-4}$) of doubly charged

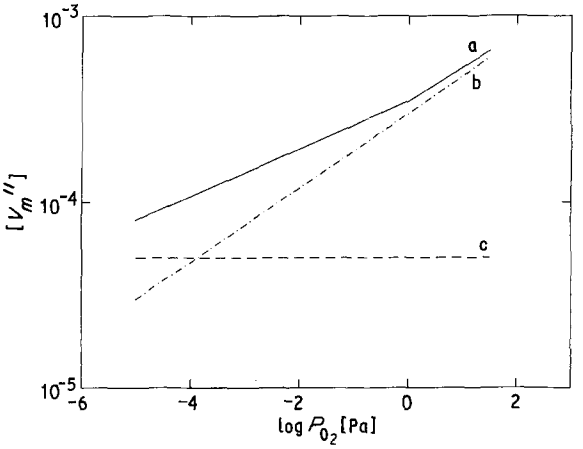

Figure 8 Extrinsic cation vacancy concentration plotted against P_{O_2} for 4300 p.p.m. iron, T = 1400° C, (a $[V''_m]_{tot}$, b $[V''_m]_{Fe}$, c $[V''_m]_{imp}$).

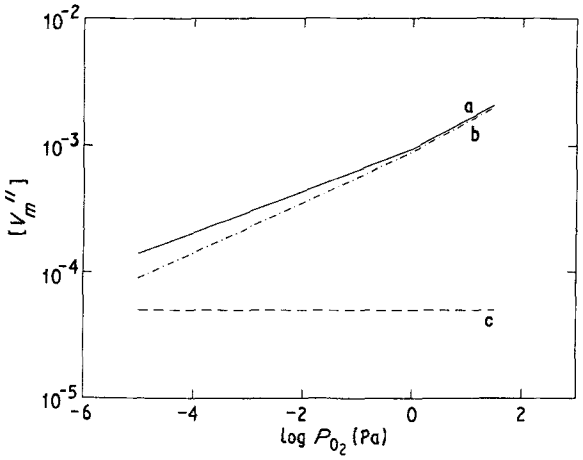

Figure 9 Extrinsic cation vacancy concentration plotted against P_{O_2} for 11 900 p.p.m. iron. T = 1400° C, (a $[V_m'']_{tot}$, b $[V_m'']_{Fe}$, c $[V_m'']_{imp}$).

vacancies compensated by electron holes. The P_{O_2} dependence of the cation vacancy concentration for a non-stoichiometric semiconducting oxide solid solution has been worked out in detail by Dimos [24].

Cation vacancies are formed through the quasi-chemical defect reaction

$$\tfrac{1}{2}O_{2(g)} + 2Fe_{Mg}^{x} = V_{Mg}'' + 2Fe_{Mg}^{\cdot} + O_O^x \quad (6)$$

The equilibrium constant for this reaction is

$$\frac{[Fe_{Mg}^{\cdot}]^2[V_{Mg}''][O_O^x]}{[Fe_{Mg}^{x}]^2 P_{O_2}^{1/2}} = K \quad (7)$$

where the square brackets indicate concentrations and x corresponds to a neutral charge. Since the concentration of O_O^x is large in comparison to the point defect concentrations, it is essentially independent of the defect concentrations and hence approximately constant. For $P_{O_2} < 1$ Pa, $[Fe_{Mg}^{x}]/[Fe_{Mg}]_{tot} > 0.9$ [27] so that $[Fe_{Mg}^{x}]$ is also approximately constant for a fixed dopant level. In this limit, the dependence of the concentration of doubly ionized cation vacancies on P_{O_2} and $[Fe_{Mg}]_{tot}$ can be obtained by combining Equations 5 and 7 to yield

$$[V_{Mg}''] \propto P_{O_2}^{1/6}[Fe_{Mg}^{x}]^{2/3} \simeq P_{O_2}^{1/6}[Fe_{Mg}]_{tot}^{2/3} \quad (8)$$

at constant temperature, total pressure, and mole fraction of MgO. At the highest P_{O_2} used in the present study (10^2 Pa), $[Fe_{Mg}^{x}]/[Fe_{Mg}]_{tot} \approx 0.65$. In this case the approximation that $[Fe_{Mg}^{x}]$ is constant breaks down and $[V_{Mg}'']$ becomes less sensitive to P_{O_2} than the one-sixth power given by Equation 8. For the present analysis, Equation 8 will be used because most of our experiments were carried out at P_{O_2} of less than 1 Pa.

At a fixed temperature, if the P_{O_2} at the surface is suddenly changed, the cation vacancy concentration at the surface will change almost instantly to the new equilibrium concentration given by Equation 8. Hence, a flux of cation vacancies between the surface and the bulk will be established to allow the cation vacancy concentration in the bulk to reach the new equilibrium concentration. If the creation or annihilation of defects at the surface or at dislocations in the bulk is not rate-controlling, then the diffusion of the cation vacancies will control the rate at which equilibrium is reached. The chemical vacancy diffusion coefficient $\tilde{D}_V$, which characterizes the migration of the vacancies in the presence of a vacancy concentration gradient, is related to the self-diffusion coefficient for cation vacancies, D_V, by the following equation:

$$\tilde{D}_V = (1 + z)D_V \quad (9)$$

where z is the degree of ionization of the cation vacancies. For the present case, $z = 2$ [27].

The rate of equilibration in terms of $\tilde{D}_V$ and the sample dimensions can be found by solving Fick's second law with the appropriate boundary conditions. The equilibration rate is described by an exponential function with a characteristic time, τ [29, 30]

$$\tau^{-1} = [\pi^2\tilde{D}_V/4][1/a^2 + 1/b^2] \quad (10)$$

where $2a$ and $2b$ are the cross-section dimensions of the sample.

The value of the chemical diffusivity at the temperature, P_{O_2}, and total iron concentration used for our experiments has been estimated in the following manner. Tracer diffusion data for iron in (Mg, Fe)O single crystals at relatively high iron concentrations and low temperatures [31] were extrapolated to the conditions used in our experiments; the cation vacancy concentration was taken to be 1% of the total iron concentration. The approximation yields a relaxation time of 1 h for a sample with dimensions of 2 mm × 2 mm at 1400° C and an iron concentration of 10 000 p.p.m. Assuming that 3τ is long enough for a sample to reach thermodynamic equilibrium a minimum annealing time of 3 h is required at 1400° C. In the present study annealing times after a change in P_{O_2} ranged from 3 to 5 h, and thus thermodynamic equilibrium should have been achieved. To check whether equilibrium was reached, one of the MgO samples with the highest iron concentration was subjected to changes in P_{O_2} during deformation at 1500° C with reequilibration times of 3 to 5 h. As in the case of the 1400° C deformation experiments, the steady-state creep rates of the 1500° C runs were insensitive to P_{O_2}.

Since the extrinsic cation vacancies are dominantly due to Fe^{+3} rather than the trivalent cation impurities and since thermodynamic equilibrium was attained after a change in P_{O_2}, the experimental results given in Equation 2 can be interpreted in terms of a possible rate-controlling mechanism for the creep of (Mg, Fe)O single crystals. The stress exponent, $n = 3.4 \pm 0.3$, and the activation energy for creep, $Q = 445 \pm 15$ kJ mol^{-1}, are both within the previously reported experimental ranges. The large value of n confirms that dislocation motion controls the deformation [1–6].

The lack of dependence of steady-state creep rate on P_{O_2} and iron concentration is consistent with the results of the high-temperature yield strength studies of Moon and Pratt [15] and Reppich [16] on iron-doped MgO. Also, Lessing [32] has shown that the steady-state strain rate of large-grained polycrystalline MgO doped with 5 300 p.p.m. iron deformed in a region of dislocation creep is insensitive to P_{O_2} [32]. As in the present investigation, the stress exponent and the activation energy for creep were nearly the same for undoped and iron-doped polycrystalline MgO.

5.2. Creep models

If the creep of (Mg, Fe)O is climb-controlled, the

rate-limiting step is expected to be the diffusion of oxygen to jogs on the dislocations. Oxygen diffusion can occur by transport through the lattice and along dislocation cores. At high temperatures and low stresses, lattice diffusion is dominant. At lower temperatures, or higher stresses, core diffusion dominates. The low value of the stress exponent (≈ 3) over the temperature and stress range investigated in this study suggests that the creep experiments were conducted in a region where lattice diffusion of oxygen is dominant. Theory predicts that n goes to $n + 2$ when control of the deformation shifts from lattice diffusion to core diffusion [33]. If the creep experiments were conducted in a region where core diffusion of oxygen was dominant, then the predicted value of n in the region where lattice diffusion of oxygen should dominate would be approximately unity, which is inconsistent with the n values for deformation controlled by dislocation climb.

For creep that is climb-controlled, the creep rate is related to the concentration of point defects responsible for oxygen diffusion and thus may be dependent on the oxygen partial pressure and concentration of iron, Equation 8. The dependence of the concentration of oxygen vacancies and oxygen interstitials on P_{O_2} and $[Fe_{Mg}]_{tot}$ can be calculated using the dependence of the concentration of doubly ionized cation vacancies on P_{O_2} and $[Fe_{Mg}]_{tot}$ given by Equation 8 plus the Schottky and Frenkel disorder reactions. The charged oxygen vacancies can be related to the charged cation vacancies through the Schottky disorder reaction

$$V_O^{\cdot\cdot} + V_{Mg}'' = \text{null}; \tag{11}$$

the mass action law for this equation is

$$[V_O^{\cdot\cdot}][V_{Mg}''] = k_s(T) \tag{12}$$

where k_s is the Schottky equilibrium constant. The doubly charged oxygen interstitials can be related to the charged oxygen vacancies through the Frenkel disorder reaction

$$O_i'' + V_O^{\cdot\cdot} = O_O^x; \tag{13}$$

the mass action law for this reaction is

$$[O_i''][V_O^{\cdot\cdot}] = k_f(T) \tag{14}$$

where k_f is the Frenkel equilibrium constant. Using Equation 8 with Equations 12 and 14, the P_{O_2} dependence of the oxygen vacancy and interstitial concentrations are

$$[V_O^{\cdot\cdot}] \propto P_{O_2}^{-1/6}[Fe_{Mg}]_{tot}^{-2/3} \tag{15}$$

and

$$[O_i''] \propto P_{O_2}^{1/6}[Fe_{Mg}]_{tot}^{2/3} \tag{16}$$

It is also possible for oxygen vacancies and interstitials to be singly charged or neutral. The defect reactions for the formation of singly ionized or neutral oxygen vacancies and interstitials may be written as follows. For vacancies,

$$V_O^{\cdot\cdot} + Fe_{Mg}^x = V_O^{\cdot} + Fe_{Mg}^{\cdot} \tag{17}$$

and

$$\tfrac{1}{2}O_2 + V_O^x = O_O^x \tag{18}$$

For interstitials,

$$O_i' + V_O^{\cdot} = O_O^x \tag{19}$$

and

$$O_i^x + V_O^x = O_O^x \tag{20}$$

Using the charge neutrality condition, $[Fe_{Mg}^{\cdot}] = 2[V_{Mg}'']$, and Equation 8 with Equations 17–20, the P_{O_2} dependence of the singly ionized and neutral oxygen vacancy and interstitial concentrations are

$$[V_O^{\cdot}] \propto P_{O_2}^{-1/3}[Fe_{Mg}]_{tot}^{-1/3} \tag{21}$$

$$[V_O^x] \propto P_{O_2}^{-1/2} \tag{22}$$

and

$$[O_i'] \propto P_{O_2}^{1/3}[Fe_{Mg}]_{tot}^{1/3} \tag{23}$$

$$[O_i^x] \propto P_{O_2}^{1/2} \tag{24}$$

If oxygen transport is through the lattice in MgO via oxygen vacancies or interstitials, the creep rate should be proportional to $P_{O_2}^m$, where $|m|$ should be $> \frac{1}{6}$ and for charged oxygen defects the creep rate is also proportional to $[Fe_{Mg}]_{tot}^q$, where $|q| \leqslant \frac{2}{3}$. Experimentally, the steady-state creep rate is observed to be proportional to $P_{O_2}^0$ and $[Fe_{Mg}]_{tot}^0$ with an activation energy of 445 kJ mol^{-1}. Therefore, it appears unlikely that the creep rate is controlled by oxygen diffusion via an extrinsic free vacancy or interstitial mechanism.

To explain their observation that oxygen self-diffusion is insensitive to the dopant level for crystals doped with oxygen, 310, and 2300 p.p.m. iron at temperatures between 1400 and 1700° C, Ando *et al.* [34] proposed an alternative mechanism in which oxygen migrates through the lattice via neutral vacancy pairs. The formation reaction for a neutral vacancy pair from Schottky-type free vacancies is

$$V_{Mg}'' + V_O^{\cdot\cdot} = (V_{Mg}''V_O^{\cdot\cdot})^x \tag{25}$$

The mass action law for this equation is

$$\frac{[V_{Mg}''V_O^{\cdot\cdot}]^x}{[V_{Mg}''][V_O^{\cdot\cdot}]} = zk_b(T) \tag{26}$$

where z is the number of orientations of the pair which contribute to the configurational entropy [34] and k_b is the equilibrium constant for Equation 26, which is related to the binding energy of the pair. Combining Equations 26 and 12 yields

$$[V_{Mg}''V_O^{\cdot\cdot}]^x = zk_b(T)k_s(T) \tag{27}$$

Thus, the concentration of vacancy pairs is a function of temperature (and of course, total pressure) but is independent of the oxygen partial pressure and the impurity concentration. Henriksen *et al.* [35] also observed that oxygen self-diffusion is insensitive to dopant concentration for MgO single crystals doped with 550 and 1400 p.p.m. trivalent cation scandium (Sc^{+3}) at a temperature of 1500° C. The dominance of the vacancy pair diffusion mechanism over the free oxygen vacancy mechanism requires that the concentration of vacancy pairs be greater than that of the single oxygen vacancies, because the migration energy of a vacancy pair is higher than or similar to that of a single oxygen vacancy [34]. For an Fe^{+3} concentration as low as 1 p.p.m., Ando *et al.* [34] concluded that the concentration of vacancy pairs is much greater than the concentration of free oxygen vacancies up to a temperature of 2000° C. An increase in the Fe^{+3} concentration increases the concentration of vacancy pairs relative to the concentration of single oxygen vacancies.

Although the lack of dependence of creep rate on oxygen partial pressure and iron concentration is consistent with a climb-controlled mechanism in which oxygen diffusion occurs by a vacancy pair mechanism (Equation 27), the discrepancy between the activation energy for oxygen self-diffusion (330 kJ mol^{-1} [36]) and that for creep (445 kJ mol^{-1}) is in marked contrast to the equality between these activation energies which is suggested by theory and observed for metals [37]. One explanation for the discrepancy between self-diffusion and creep activation energies has been proposed to explain the high-temperature creep results for (Mg, Fe)$_2$SiO$_4$ [38] Co$_2$SiO$_4$ [39], Fe$_2$SiO$_4$ [39], and V-doped Mg$_2$SiO$_4$ [25]. The rate of climb of an edge dislocation, v_c, is proportional to the velocity of jogs along the dislocation, v_j, times the concentration of jogs c_j;

$$v_c \propto c_j v_j \tag{28}$$

In local thermodynamic equilibrium, the concentration of jogs is given by

$$c_j = \exp(-U_j/kT) \tag{29}$$

where U_j is the jog formation energy [40]. The velocity of the jogs is proportional to the rate of diffusion,

$$v_j \propto D \propto \exp(-Q_d/kT) \tag{30}$$

where Q_d is the activation energy for diffusion of the slowest moving species. Thus, the activation energy for dislocation climb, Q_c, is composed of two terms,

$$Q_c = Q_d + U_j \tag{31}$$

For metals, U_j is generally believed to be small so that the dislocation acts as a perfect source/sink for point defects [41]. However, in oxides and silicates, the formation energy for jogs appears to be on the order of the activation energy for self-diffusion. In this model, then, the rate of creep of (Mg, Fe)O crystals is controlled by the nucleation and motion of jogs along edge dislocations: The jog nucleation process involves an energy of approximately 115 kJ mol^{-1} ($U_j = Q_c - Q_d$ = 445 kJ mol^{-1}–330 kJ mol^{-1}), and the rate of motion of the jogs is limited by oxygen diffusion via a vacancy pair mechanism. This argument is consistent with the fact that the activation energy determined by Narayan and Washburn [42] from dislocation loop shrinkage (climb) studies, 460 kJ mol^{-1}, is much greater than the activation energy for oxygen self-diffusion in MgO determined using tracer techniques, $\approx$330 kJ mol^{-1} [36], but is similar to the activation energy for creep, 445 kJ mol^{-1}.

Acknowledgement

This research was supported by the National Science Foundation through grants DMR-8100131 and DMR-8500480.

References

1. R. L. CUMMEROW, *J. Appl. Phys.* **34** (1963) 1724.
2. W. S. ROTHWELL and A. S. NEIMAN, *ibid.* **36** (1965) 2309.
3. *Idem, Appl. Phys. Lett.* **3** (1963) 160.
4. C. O. HULSE and J. A. PASK, *J. Amer. Ceram. Soc.* **43** (1960) 373.
5. P. C. DOKKO and J. A. PASK, *ibid.* **62** (1979) 433.
6. W. HUETHER and B. REPPICH, *Phil. Mag.* **28** (1973) 363.
7. J. M. BIRCH and B. WILSHIRE, *ibid.* **30** (1974) 1023.
8. *Idem., ibid.* **31** (1975) 1421.
9. A. H. CLAUER and B. A. WILCOX, *J. Amer. Ceram. Soc.* **59** (1976) 89.
10. A. H. CLAUER, M. S. SELTZER and B. A. WILCOX, *ibid.* **62** (1979) 85.
11. J. L. ROUTBORT, *Acta Metall.* **27** (1979) 649.
12. P. J. DIXON-STUBBS and B. WILSHIRE, *Trans. Brit. Ceram. Soc.* **79** (1980) 21.
13. J. B. BILDE-SORENSON, *J. Amer. Ceram. Soc.* **55** (1972) 606.
14. B. ILSCHNER and B. REPPICH, in "Defects and Transport in Oxides", edited by M. S. Seltzer and R. I. Jaffe (Plenum, New York, 1975) p. 425.
15. R. L. MOON and P. L. PRATT, *Proc. Brit. Ceram. Soc.* **15** (1976) 203.
16. B. REPPICH, *Mater. Sci. Engng* **22** (1976) 71.
17. J. M. VIEIRA and R. J. BROOK, in "Structure and Properties of MgO and Al_2O_3 Ceramics", edited W. D. Kingery (American Ceramics Society Inc., Columbus, 1984) p. 438.
18. G. W. GROVES and M. E. FINE, *J. Appl. Phys.* **35** (1964) 3587.
19. R. W. DAVIDGE, *J. Mater. Sci.* **2** (1967) 339.
20. M. SRINVASAN and T. G. STOEBE, *J. Appl. Phys.* **41** [9] (1970) 3726.
21. E. W. KRUSE and M. E. FINE, *J. Amer. Ceram Soc.* **55** (1972) 32.
22. W. E. LUECKE and D. L. KOHLSTEDT, *Ibid.* **71** (1988) 189.
23. K. W. BLAZEY, *J. Phys. Chem. Solids* **38** (1977) 671.
24. D. DIMOS, PhD Thesis, Cornell University, Ithaca (1986).
25. S. J. MACKWELL and D. L. KOHLSTEDT, *Phys. Chem. Min.* **13** (1986) 351.
26. D. L. RICOULT and D. L. KOHLSTEDT, *J. Amer. Ceram. Soc.* **69** (1986) 770.
27. W. H. GOURDIN, W. D. KINGERY and J. DRIER, *J. Mater. Sci.* **14** (1979) 2074.
28. G. W. HOLLENBERG and R. S. GORDON, *J. Amer. Ceram. Soc.* **56** (1973) 140.
29. J. CABRERA-CANO, A. DOMINIGUEZ-RODRIGUEZ, R. MARQUEZ, J. CASTAING and J. PHILIBERT, *Phil. Mag.* **46** (1982) 397.
30. S. J. MACKWELL, D. B. DIMOS and D. L. KOHLSTEDT, *ibid.* **A57** (1988) 779.
31. W. K. CHEN and N. L. PETERSON, *J. Phys. Chem. Solids* **41** (1980) 335.
32. P. A. LESSING, PhD Thesis, University of Utah, Salt Lake City (1976).
33. K. C. GORETTA and J. C. ROUTBORT, *Acta Metall.* **35** (1987) 1047.
34. K. ANDO, Y. KUROKAWA and Y. OISHI, *J. Chem. Phys.* **78** (1983) 6890.
35. A. F. HENRIKSEN, Y. M. CHIANG, W. D. KINGERY and W. T. PETSUKEY, *J. Amer. Ceram. Soc.* **66** (1983) C144.
36. L. E. DOHLERT, PhD Thesis, Massachusetts Institute of Technology, Boston (1985).
37. J. WEERTMAN, Trans. ASM 61 (1968) 681.
38. D. L. KOHLSTEDT and D. L. RICOULT, in "Plastic Deformation of Ceramic Materials" edited R. C. Bradt and R. E. Tressler (Plenum, New York, 1974) p. 251.
39. D. L. RICOULT and D. L. KOHLSTEDT, *Phil. Mag.* **A51** (1985) 79.
40. J. FRIEDEL, "Dislocations" (Pergamon, Oxford, 1964).
41. R. W. BALLUFFI and A. V. GRANATO, in "Dislocations in Solids", edited F. R. N. Nabarro (North-Holland, New York 1979) Vol. 4, p. 1.
42. J. NARAYAN and J. WASHBURN, *Acta Metall.* **21** (1973) 533.

Received 14 August
and accepted 1 December 1987